Virchows Arch (2009) 454:89–99
DOI 10.1007/s00428-008-0697-3

ORIGINAL ARTICLE

Renal angiomyoadenomatous tumor: morphologic, immunohistochemical, and molecular genetic study of a distinct entity

M. Michal · O. Hes · J. Nemcova · R. Sima · N. Kuroda · S. Bulimbasic · M. Franco · N. Sakaida · D. Danis · D. V. Kazakov · C. Ohe · M. Hora

Received: 11 May 2008 / Revised: 26 September 2008 / Accepted: 29 October 2008 / Published online: 20 November 2008

Abstract We present a series of a distinct tumorous entity named renal angiomyoadenomatous tumor (RAT). Five cases were retrieved from the consultation files of the authors. Histologic and immunohistochemical features were evaluated. Sequencing analysis of coding region of the VHL gene was carried out in all cases. The tumors were composed of admixture of an epithelial clear cell component and prominent leiomyomatous stroma. Epithelial cells formed adenomatous tubular formations endowed with blister-like apical snouts. All tubular/glandular structures were lined by a fine capillary network. The epithelial component was positive for epithelial membrane antigen, CK7, CK20, AE1-AE3, CAM5.2, and vimentin in all cases. In all analyzed samples, no mutation of the VHL gene was found. RAT is a distinct morphologic entity, being different morphologically, immunohistochemically, and genetically from all renal tumors including conventional clear cell carcinoma and mixed epithelial and stromal tumor of kidney.

Keywords Renal angiomyoadenomatous tumor · Mixed epithelial and stromal tumor · Leiomyomatous stroma · Kidney

Introduction

Renal angiomyoadenomatous tumor (RAT) is a recently described neoplasm microscopically characterized by leiomyomatous stroma often forming abortive vascular structures surrounding and encasing a distinctive epithelial component [18]. Since the time we published a case of RAT, we have been receiving in consultation putative cases of RAT with the request to confirm or exclude the

M. Michal · O. Hes · J. Nemcova · R. Sima · D. V. Kazakov
Department of Pathology,
Charles University, Faculty Hospital,
Plzen, Czech Republic

M. Hora
Department of Urology,
Charles University, Faculty Hospital,
Plzen, Czech Republic

N. Kuroda
Red Cross Hospital Kochi,
Kochi, Japan

N. Sakaida · C. Ohe
Department of Pathology,
Kansai Medical University Hirakata Hospital,
Osaka, Japan

S. Bulimbasic
University Hospital Dubrava,
Zagreb, Croatia

M. Franco
EPM/UNIFESP,
Sao Paulo, Brazil

D. Danis
Cytopathos s.r.o.,
Bratislava, Slovakia

M. Michal (✉)
Sikl's Department of Pathology,
Laboratore Spec. Diagnostiky Medical Faculty Hospital,
Charles University,
Alej Svobody 80,
304 60 Plzen, Czech Republic
e-mail: michal@medima.cz

diagnosis. This resulted in identification of five new cases of RAT, which clinicopathologic and genetic features are presented herein.

Materials and methods

The five cases of RAT were collected from the files of the Charles University Hospital Plzen in the Czech Republic, the Red Cross Hospital Kochi (originated from Kansai Medical School Hirakata Hospital) in Japan, the University Hospital Dubrava in Zagreb in Croatia, the EPM/UNIFESP Sao Paulo in Brazil, and Cytopathos s.r.o. Bratislava in the Slovak Republic.

Histologic sections of formalin-fixed, paraffin-embedded tissue were stained with hematoxylin and eosin. Primary antibodies to the following antigens were employed: cytokeratins CK7 and 8 (clone CAM5.2, at 1:50, Becton-Dickinson, San Jose, CA, USA), Pancytokeratin (clone AE1-AE3, at 1:500, Boehringer, Mannheim, Germany), CK7 (clone OV-TL 12/30, at 1:200, DakoCytomation, Glostrup, Denmark), CK20 (clone K20.8, at 1:1,000, Neomarkers, Fremont, CA, USA), epithelial membrane antigen (EMA; clone E29, at 1:1,000, DakoCytomation), carbonic anhydrase IX (R&D Systems, Minneapolis, MN, USA; clone 303123, at 1:500), Ki-67 (clone MIB1, at 1:200, DakoCytomation), HMB45 (clone HMB45, at 1:300, DakoCytomation), S100 protein (polyclonal, at 1:200, Novocastra, Newcastle, UK), TFE3 (polyclonal, at 1:500, Santa Cruz Biotechnology, Santa Cruz CA, USA), CD34 (clone QBEnd10 at 1:800, Neo-Markers), CD117 (polyclonal, at 1:150, NeoMarkers), vimentin (clone V9, at 1:1,000, Neomarkers), racemase (clone P504S, at 1:3,500, Assay Design, Ann Arbor, MI, USA), smooth muscle actin (clone 1A4, at 1:1,000, DakoCytomation), desmin (clone D33, at 1:3,000, DakoCytomation), caldesmon (clone h-CD, at 1:50, DakoCytomation), calponin (clone CALP, at 1:1,000, DakoCytomation) and factor VIII (polyclonal, at 1:4,000, DakoCytomation), tyrosinase (clone T311, at 1:400, DakoCytomation), and Melan A (clone A103, at 1:400, DakoCytomation). The primary antibodies were visualized using the supersensitive streptavidin–biotin–peroxidase complex (BioGenex, San Ramon, CA, USA).

Analysis of VHL gene mutation and 3p loss of heterozygosity

Five 10-μm thick sections of tumor tissue were cut from formalin-fixed, paraffin-embedded blocks. Epithelial and smooth muscle components were manually microdissected. DNA was extracted separately from each component by the NucleoSpin Tissue Kit (Macherey Nagel, Duren, Germany) according to manufacturer's protocol. Polymerase chain reaction (PCR) for the VHL gene analysis was carried out using primers displayed in Table 1. PCR for loss of heterozygosity (LOH) analysis of chromosome 3p was performed using short tandem repeat (STR) markers and primers shown in Table 2. Normal tissues of the same patients were used as a reference. The reaction conditions were as follows: 12.5 μl of HotStart Taq PCR Master Mix (QIAgen, Hilden, Germany), 10 pmol of each primer, 100 ng of template DNA, and distilled water up to 25 μl. Amplification program for all fragments, except the marker D3S666, consisted of denaturation at 95°C for 15 min, then 40 cycles of denaturation at 95°C for 1 min, annealing at 55°C for 1 min, and extension at 72°C for 1 min. The program was finished by 72°C incubation for 7 min. Annealing temperature for fragment D3S666 was 58°C.

Successfully amplified PCR products of the VHL gene were purified with a Montage PCR Centrifugal Filter Devices (Millipore, Billerica, MA, USA) and sequenced using a Big Dye Terminator Sequencing kit (PE/Applied Biosystems, Foster City, CA, USA). Samples were then run on an automated sequencer ABI Prism 310 (PE/Applied Biosystems) at a constant voltage of 11.3 kV for 20 min. Successfully amplified PCR products of STR markers were mixed with a size marker and run on an automated sequencer ABI Prism 310 (PE/Applied Biosystems) at a constant voltage of 15 kV for 28 min.

Ultrastructure

Formalin-fixed wet material from one case was available for ultrastructural analysis. The formalin-fixed sample was postfixed in 2% glutaraldehyde, contrasted in 1% osmium tetroxide, and embedded in epoxy resin (Durcupan-Epon). Semithin sections were cut, stained with toluidine blue, and examined by light microscopy. Thin sections from representative areas were then cut, stained with uranyl acetate and lead citrate, and examined with a Philips (Eindhoven, Holland) EM208S transmission electronic microscope.

Small pieces of paraffin-embedded tissues were obtained from additional two cases. Tissues were deparaffinized according protocol of Widéhn and Kindblom and reprocessed for ultrastructure examination [22].

Results

Clinical features

The basic clinicopathologic data of the patients are summarized in Table 3.

Four out of the five patients with RAT were men, and one patient was a woman. The age of the patients ranged

Table 1 Primers for amplification and sequencing of the VHL gene

Exon	Name	Sequence 5′ → 3′	Reference
Exon 1	VHL e1–1	CGCGAAGACTACGGAGGT	New primers
	VHL e1–2	GTCTTCTTCAGGGCCGTA	
	VHL e1–3	GAGGCAGGCGTCGAAGAG	
	VHL e1–4	GCGATTGCAGAAGATGACCT	
	VHL e1–5	GCCGAGGAGGAGATGGAG	
	VHL e1–6	CCCGTACCTCGGTAGCTGT	
	VHL e1–7	CCGTATGGCTCAACTTCGAC	
	VHL e1–8	GCTTCAGACCGTGCTATCGT	
Exon 2	VHL e2–1	ACCGGTGTGGCTCTTTAACA	New primers
	VHL e2–2	TCCTGTACTTACCACAACAACCTT	
Exon 3	VHL e3–1	GATTTGGTTTTTGCCCTTCC	Michal et al. [17]
	VHL e3–2	ACATTTGGGTGGTCTTCCAG	
	VHL e3–3	CGTCAGGTCGCTCTACGAA	
	VHL e3–4c	CCATCAAAAGCTGAGATGAAAC	

from 49 to 93 years (mean 64.6 years). None of the patients had signs of tuberous sclerosis. The female patient had adenocarcinoma of sigmoid colon diagnosed 1 year before nephrectomy for the RAT. The kidney tumor was discovered during a regular check-up oncologic examination; it remained unknown whether the renal tumor was present already at the time of abdominal surgery for the adenocarcinoma of the colon. The adenocarcinoma of the colon recurred 1 year after the nephrectomy, and the recurrence was surgically excised. Twenty-nine months after the nephrectomy, the patient died of metastatic colonic adenocarcinoma without recurrence of RAT. Of the remaining four patients, three were alive and well at 8, 9, and 12 months, and one patient was lost to follow-up.

Gross findings

The largest dimensions of RATs ranged from 2.3 to 8.5 cm (mean 4.1 cm). The renal pelvis, renal veins, and sinus were not involved by any of the tumors. Grossly, RATs were grayish or tan to light brown in color (Fig. 1a). The tumors were sharply circumscribed with a variously thick capsule.

Table 2 Primers for amplification of STR markers for LOH 3p analysis

STR marker	Sequence 5′ → 3′
D3S1317	TACAAGTTCAGTGGAGAACC
	CCTCCAGGCCATACACAGTCA
D3S1300	AGCTCACATTCTAGTCAGCCT
	GCCAATTCCCCAGATG
D3S666	CAAGGCATTAAAGTGGCCACGC
	GTTTGAACCAGTTTCCTACTGAG
D3S1768	GGTTGCTGCCAAAGATTAGA
	CACTGTGATTTGCTGTTGGA

Microcystic change was apparent in all cases. One case revealed marked cystic changes (Fig. 1b). There were no grossly apparent necroses; however, patchy hemorrhagic areas were frequent.

Microscopic findings

Histologically, all tumors had a variously thick capsule formed by a layer of bands of smooth muscle (Fig. 2). All tumors were characterized by the intimate intermixture of an epithelial component and smooth muscle tissue. The latter formed a predominant component of the tumor mass in case 3; it was prominent but not dominant in three cases and rather inconspicuous but still well developed in the remaining case 5. The epithelial tissue was represented by adenomatous structures composed of cells with small deeply basophilic nuclei, often in a linear arrangement reminding of small beads on a string (Fig. 3). The nuclei of the neoplastic cells were of equal size and small; only in case 3, there were rare cells with somewhat enlarged nuclei. Some glandular structures were more distended and contained deeply eosinophilic colloid with "moth-eaten" peripheral areas (Fig. 4). Cytologically, the nuclei of the epithelial cells in these glandular structures were irregular and manifested one to several inconspicuous nucleoli; there were many cells with variously cleaved nuclei. In a majority of the well-formed tubular or branching structures, the nuclei were in a basal position close to the basal membrane. The cytoplasm of the cells was covered by typical clear snouts, which looked like optically clear blisters and appeared as though being grafted on the luminal surface of the cells. The equal size of the secretory cells with basophilic nuclei caused by dense nuclear chromatin alienated along the basal membrane combined with the prominent apical clear snouts resulted in a focal

Table 3 Clinical features

	Sex/age	Side	Size	Follow-up
Case 1	M/58	Right	2.3×2.3×1.8 cm	9 months AW
Case 2	M/49	Left	Diameter 4.6 cm	1 year AW
Case 3	M/93	Right	8.5×8×3 cm	8 months AW, then LOF
Case 4	F/73	Left	Diameter 2.5 cm	29 months DWT[a]
Case 5	M/50	Right	Diameter 2.5 cm	LOF

F female, *M* male, *AW* alive and well, *LOF* loss on follow-up, *DWT* died without tumor
[a] Patient died of metastatic disease of colonic adenocarcinoma

but characteristic appearance of some adenomatous structures reminiscent of a "shark's smile" (Fig. 5). Focally, the lumina of the tubules were collapsed, which resulted in a solid growth pattern in these areas (Fig. 6). In other places, the tumors showed gradual (Fig. 7a) or sharp (Fig. 7b) transitions to areas with a clear cell change. Focally, these clear cell adenomatous structures grew interspersed among the adenomatous areas with basophilic nuclei (Fig. 7c).

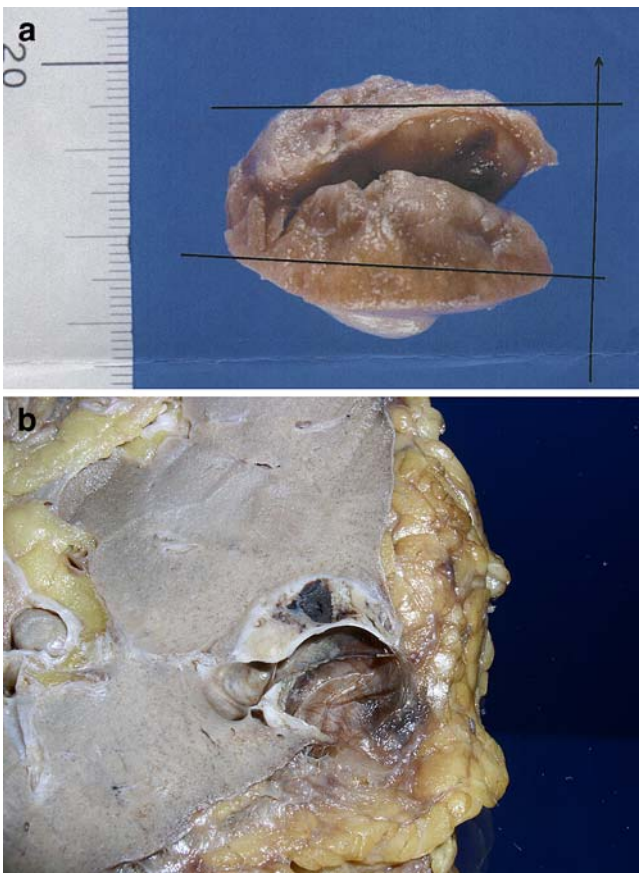

Fig. 1 The tumor is grayish or tan to light brown in color (**a**). Marked cystic changes as evident here were detected in one case (**b**)

These clear cell areas bore some resemblance to conventional clear cell carcinomas, grade 1 according to Fuhrman. In these clear cell areas, the nuclei of the neoplastic cells often lost their basal positions, and the clear snouts were much less conspicuous or entirely absent (Fig. 7d).

There was a remarkable relationship between a capillary network and the epithelial component in the sense that every single adenomatous structure of RAT, whether in the solid, tubular, or clear cell areas, was associated with a capillary network, with the capillaries intimately surrounding the circumference of the basal membrane of all adenomatous structures (Fig. 8). In those areas, in which the adenomatous structures branched and formed micropapillary projections, these capillaries formed their only supportive stroma. This capillary vasculature was often poorly recognizable in hematoxylin and eosin stained slides but was apparent with immunohistochemical stains for endothelial markers or pericytes (see below). No such capillary network was observed in ten randomly selected cases of the clear cell renal carcinoma and one case of clear cell renal carcinoma associated with leiomyomatous stroma from our files.

There were no atypias or mitoses apparent in the tumors. The stromal muscular component formed eosinophilic bundles and strands of leiomyomatous tissue composed of elongated cells with cigar-shaped nuclei when cut along the long axis. The leiomyomatous stroma grew inside the tumors among the epithelial component, and in addition, variously thick bands of leiomyomatous tissue encircled the whole tumors, forming thus a continuous capsule (Fig. 1). Focally, the leiomyomatous tissue formed abortive vessels with formations of incomplete walls with lumina, which usually lacked elastic layer, or the elastic stains showed a small amount of thin disorganized elastic fibers. The leiomyomatous tissue often entirely encased patches of adenomatous structures (Fig. 9a, b), or it formed only small leiomyomatous islands within the epithelial component (Fig. 9c). The leiomyomatous

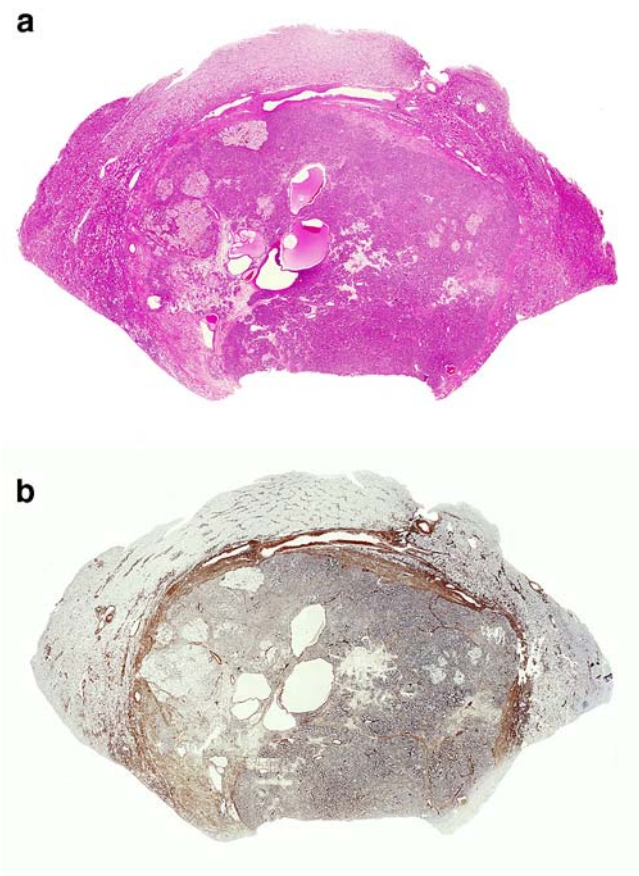

Fig. 2 **a** The tumor is surrounded by a variously thick capsule formed by a layer of bands of smooth muscle incorporating abortive angiomatous structures (hematoxylin and eosin stain). The same slide with smooth muscle actin antibody staining (**b**)

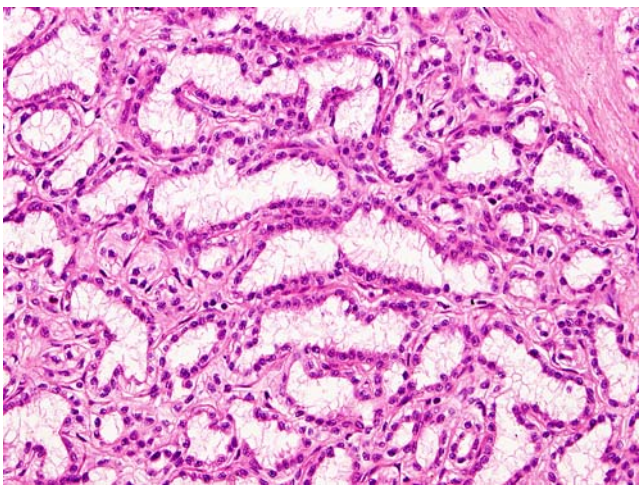

Fig. 3 The epithelial component is represented by adenomatous structures composed of cells with small deeply basophilic nuclei often in a linear arrangement reminding small beads on a string. The cytoplasm of the cells manifest clear snouts appearing like optically clear blisters at the apical surface (hematoxylin and eosin stain)

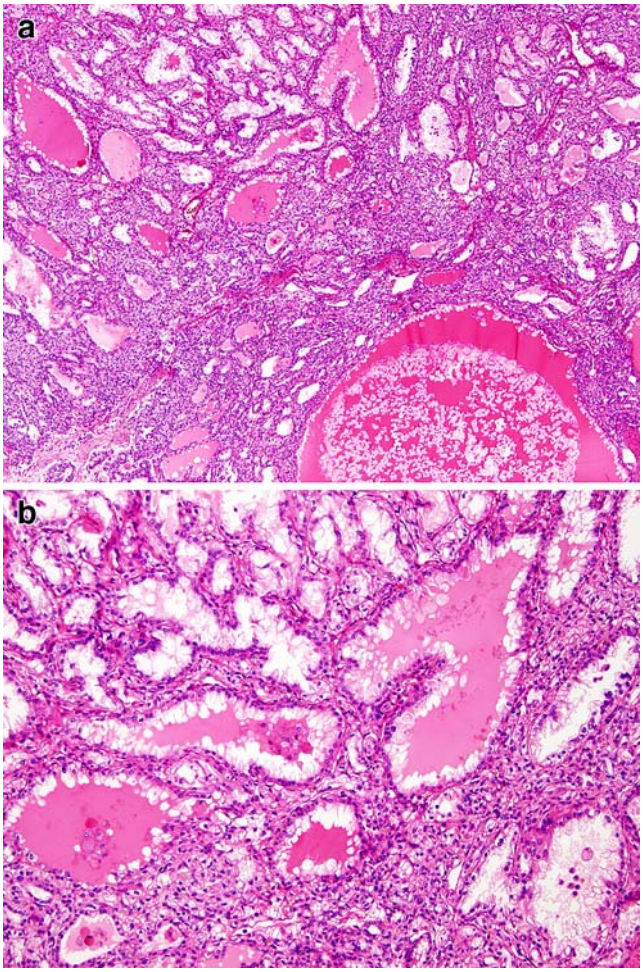

Fig. 4 Some glandular structures are distended and contain deeply eosinophilic colloid, which has a "moth-eaten" appearance at the periphery (**a**, **b**) (hematoxylin and eosin stain)

stroma frequently underwent a myxoid or hyaline change. Metaplastic ossification was noted in case 3. Adipose tissue and other tissues such as, for example, thick blood vessels devoid of elastic layer with the typical arrangement of the myoid stromal cells perpendicularly to the lumina of these vessels, that may be seen in renal angiomyolipoma (PECOMA), were not detected in our cases of RAT. Multinucleated cell granulomas or hyaline globules, which are sometimes seen in conventional clear renal cell carcinomas [8–10], were not observed in any of the tumors in our series.

Histochemical findings

Mucicarmine stain was negative throughout the tumors. Glycogen and periodic acid–Schiff (PAS) stainings showed various amounts of glycogen (digested with PAS-diastase) in the adenomatous structures including the clear snouts (Fig. 10), as the amount of glycogen in tissues depends on the time of fixation in formol.

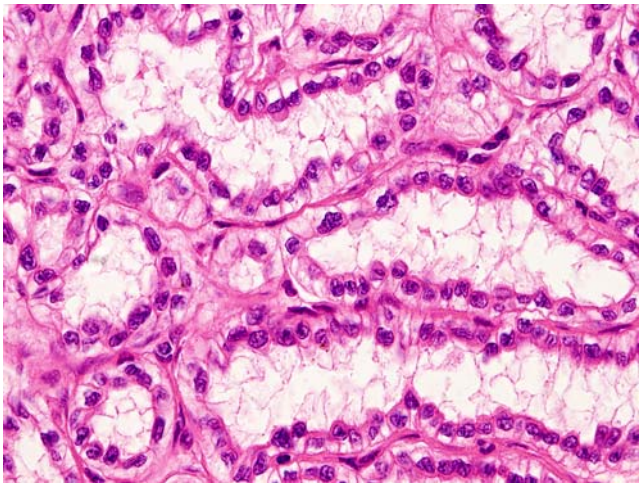

Fig. 5 The equal size of the secretory cells with basophilic nuclei alienated along the basal membrane together with prominent apical clear snouts producing a similarity to a "shark's smile" (hematoxylin and eosin stain)

Immunohistochemical findings

Immunohistochemically, the epithelial component of tumors was positive with all antibodies to cytokeratins AE1-AE3, CAM 5.2, CK 7, and CK 20. While CK7 always strongly stained all epithelial tissues, the reaction with CK20 was only weak and often focal. In addition to cytokeratin positivity, the epithelial component was strongly positive for EMA and vimentin in all cases and, unexpectedly, for tyrosinase in one case. CD10 reacted negatively in four tumors, while in the remaining case, there were rare epithelial cells that stained weakly for this marker. The epithelial component was negative with all the rest of the tested antibodies including HMB45 and Melan A. Carbonic anhydrase IX antibody reacted in the epithelial component positively and negatively in the leiomyomatous component in all five cases.

The stromal leiomyomatous component reacted positively and strongly with antibodies to caldesmon, calponin, vimentin, and smooth muscle actin in all cases, whereas immunostaining for desmin was patchy and weak. The leiomyomatous stromal component was negative with all the rest of the tested antibodies, including the melanocytic markers (HMB45, Melan A, and tyrosinase).

The endothelial cells of the capillary network were positive for FVIII and CD34 in all cases. Conspicuous positivity of the pericytic network was apparent with CD31 or smooth muscle actin stains, highlighting the intimate relationship of the capillary network with the glandular structures (Fig. 11). The proliferative index (MIB1) was generally very low, and always less than 1% of the cells reacted positively.

Electron microscopic findings

Ultrastructurally, the epithelial cells had a well-formed cytoplasmic membrane and were attached by desmosomes. The cytoplasm was rich in organelles (Golgi apparatus, lysosomes, mitochondria, and smooth endoplasmic reticulum). Nuclei were round with irregular clefts and inconspicuous nucleoli. The cytoplasm of the tumor cells formed edematous organelle-poor clear cytoplasmic snouts corresponding with the structures visible at the light microscopic level. Microvilli were present between snouts on the apical surface of epithelial cells.

The leiomyomatous cells had convoluted and intended nuclei and inconspicuous nucleoli; the cytoplasm contained well-developed endoplasmic reticulum and intermediate filaments. The ultrastructural features of the leiomyomatous component were thus identical to other benign leiomyomas.

No melanosomes (or similar structures) were detected in both cellular populations. There were no neurosecretory granules seen in the cytoplasm of the cells.

Analysis of the VHL gene mutation and 3p LOH

Molecular genetic findings are summarized in Table 4. Case no. 5 was excluded from the further analysis because of low quality of DNA. In the remaining four cases, no mutation of coding sequence of the VHL gene was found in epithelial and smooth muscle cell components of the tumors. PCR for LOH analysis of chromosome region 3p did not reveal any copy number changes in all successfully analyzed samples.

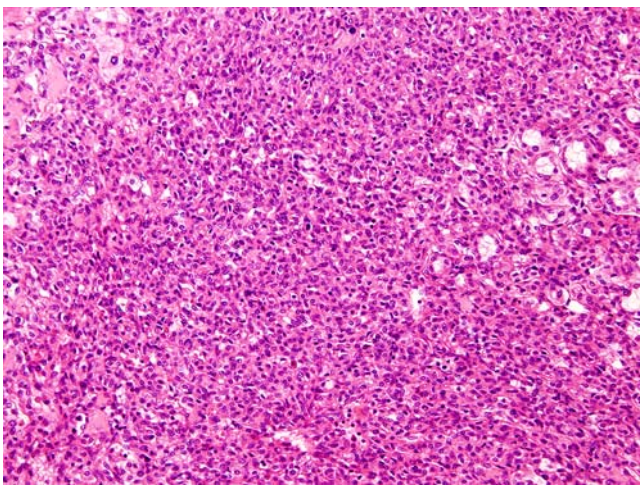

Fig. 6 Focal collapse of the lumina of the tubules resulting in a solid growth pattern in these areas (hematoxylin and eosin stain)

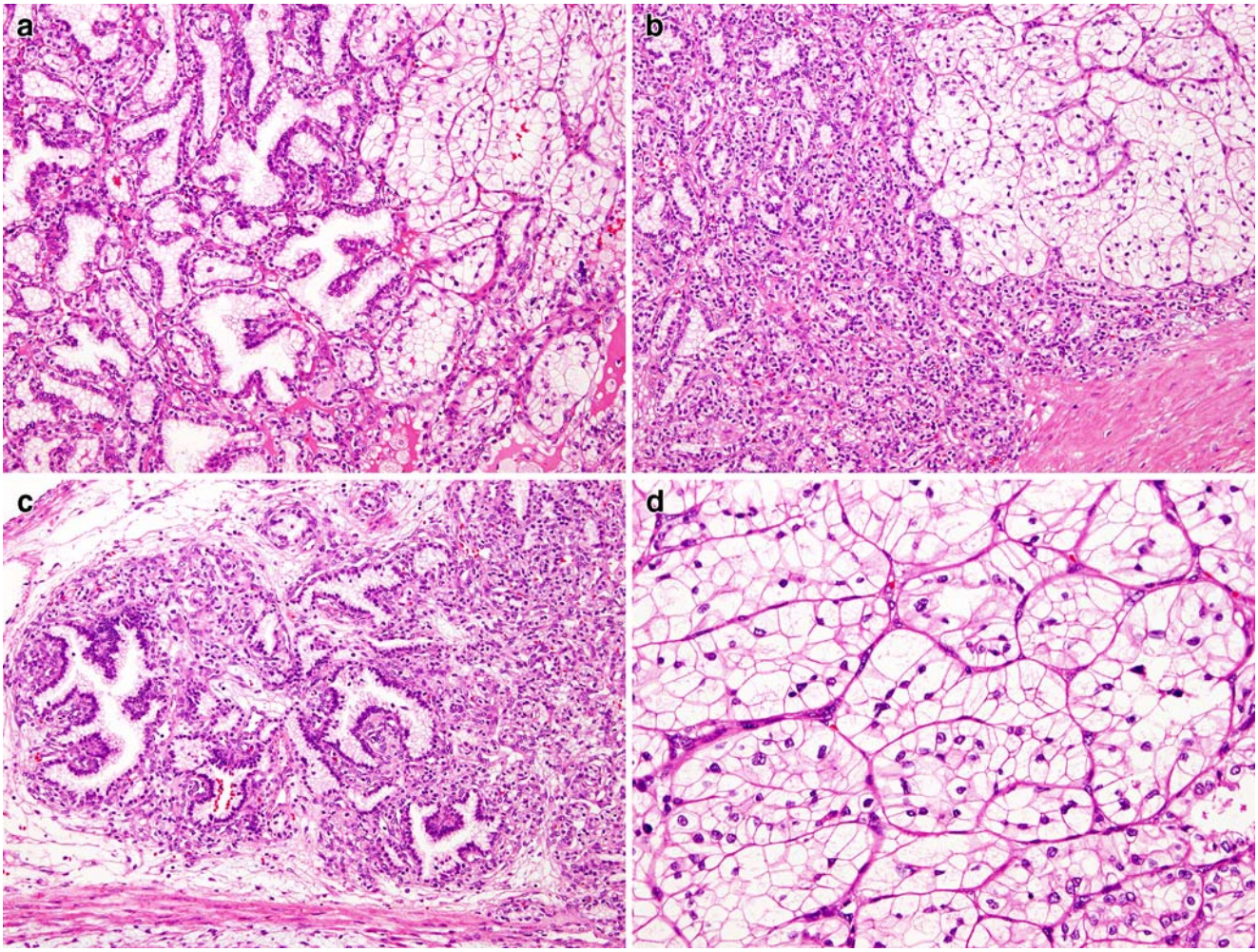

Fig. 7 Areas with a clear cell change. These transitions to clear cell areas were either gradual (**a**) or sharp (**b**). In this area, clear cell adenomatous structures are interspersed among adenomatous areas with basophilic nuclei (**c**). In the clear cell areas, the nuclei of the neoplastic cells often lost their basal positions and the clear snouts were absent (**d**) (hematoxylin and eosin stain)

Discussion

There are two types of renal tumors that manifest the characteristic epithelial and stromal components that are mixed epithelial and stromal tumors of the kidney (MESTK) and RAT. One of these two tumors, MESTK, is a recently defined entity [1, 14–16, 20, 23] which, together with cystic partially differentiated nephroblastomas and mesoblastic nephromas, used to be lumped in the past under the diagnostic term "cystic nephroma" [13]. RAT, first described by Michal et al. in 2000, is characterized by tubular to branching adenomatous structures endowed with apical clear snouts and surrounded by a capillary network and variously copious, HMB45-negative, leiomyomatous stroma focally forming abortive vascular structures [18]. We consider tyrosinase immunohistochemical positivity in the epithelial component of one case of RAT in this series to be an aberrant, however, interesting feature of the lesion.

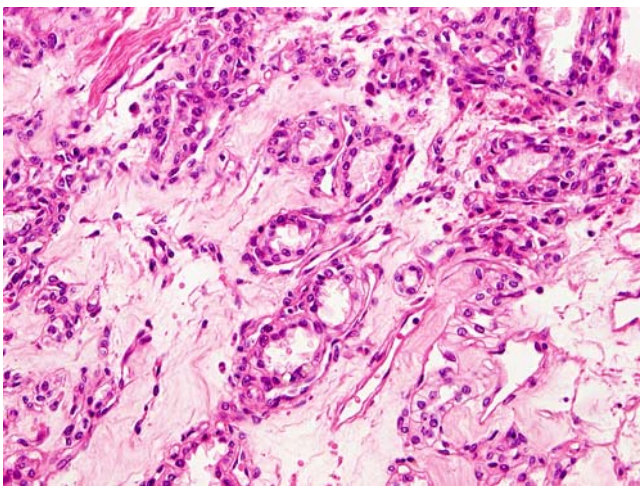

Fig. 8 Capillaries intimately surrounding the circumference of the basal membranes of adenomatous structures (hematoxylin and eosin stain)

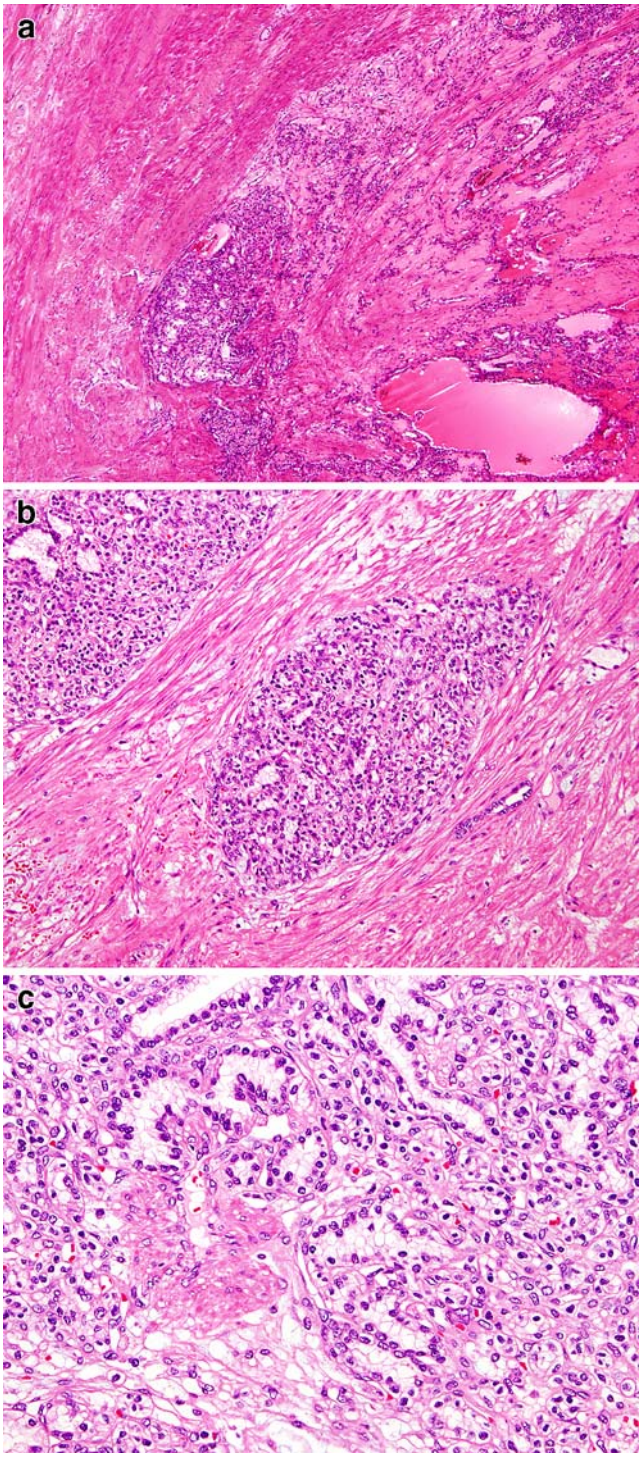

Fig. 9 Leiomyomatous stroma encasing patches of adenomatous structures (**a**, **b**) or forming only small leiomyomatous islands within the epithelial component (**c**) (hematoxylin and eosin stain)

The amount of leiomyomatous stroma in RAT is highly variable. It may range from 10% to 70% of the whole tumor mass, it forms abortive vascular structures, and notably, it lacks a lipomatous component. In our experience and according to the publication by Kuhn et al. [12], this

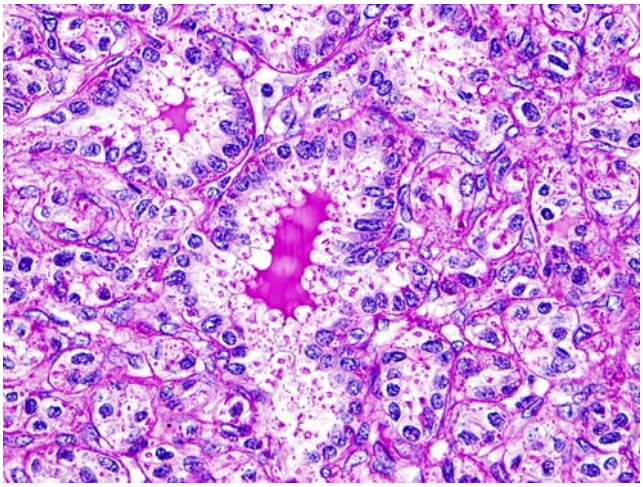

Fig. 10 PAS staining: note glycogen in glandular structures including clear snouts (PAS staining)

angioleiomyomatous stroma is not entirely specific for RAT, as it can rarely be seen in conventional renal clear cell carcinomas.

The epithelial component of RAT is unique to this tumor. The equal size of the secretory cells with basophilic nuclei lined in the basal positions and the apical clear snouts are responsible for the typical appearance of the glandular structures reminiscent of a "shark smile." The other typical feature is the fine and delicate network of capillaries surrounding every single neoplastic tubule best visible on immunohistochemical slides stained, for example, with CD31 or smooth muscle actin (Fig. 11). In our experience, the degree of this capillary networking in RAT surpasses vasculature of the renal clear cell carcinomas.

The association of the above-described epithelial component of RAT with the capillary network is also unique and can serve as a diagnostic clue. This can be illustrated

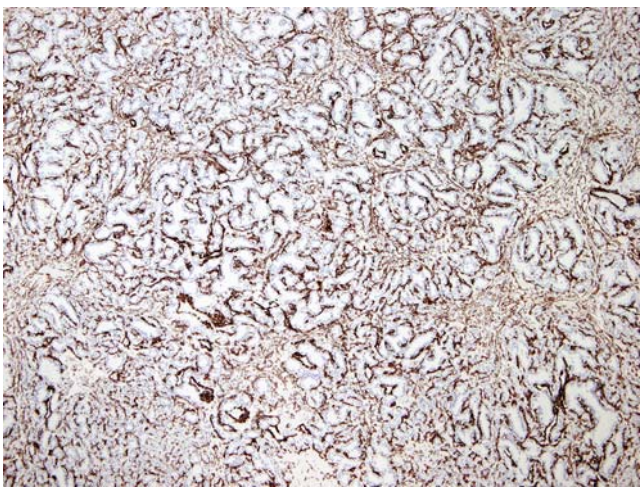

Fig. 11 Conspicuous positivity of a pericytic network (immunohistochemistry with smooth muscle actin antibody)

Table 4 Molecular genetic findings

Number of specimen	D3S1317	D3S1300	D3S666	D3S1768	VHL mutation status
No 1	Negative	NI	Negative	NA	wt/wt
No 2	Negative	Negative	Negative	Negative	wt/wt
No 3	Negative	NA	NA	NA	wt/wt
No 4	Negative	Negative	NI	Negative	wt/wt
No 5	NA	NA	NA	NA	NA

NA non-analyzable, *NI* non-informative, *wt* wild type

by case 5 of this series, from which we originally received only one tissue block, wherein there were present only glandular structures with apical snouts forming the "shark's smile" and the garland-like capillaries endowing every single tubule typical of RAT, with nearly no angioleiomyomatous stroma. Being sure that the tumor represented RAT, we asked the referring pathologist for additional tissue blocks, and tissue sections from three of the four additional blocks evidenced the typical angioleiomyomatous stroma, although in this particular case, it represented a minor component of the neoplasm, forming approximately 10% of the whole tumor mass.

There are several cases of renal cell tumors having glandular component and leiomyomatous stroma published in the literature. Honey et al. published a case of a bilateral metachronous renal cell carcinoma in an 18-year-old female patient with clinical evidence of tuberous sclerosis [11]. Beside the renal cell carcinoma, they described "an abnormally large quantity of smooth muscle, not apparently related to the pelvis or calyces, nor to blood vessels". Unfortunately, the authors provided neither description nor illustration of the relationship between these bundles and the renal cell carcinoma. Their patient was alive and well 4 years later [11]. Govaerts et al. reported a case of a 54-year-old woman with no evidence of tuberous sclerosis, which had a conventional renal cell carcinoma embedded within a mesenchymal lesion thought to be of a hamartomatous nature and called by the authors as angiofibroma [7]. No follow-up information was provided. Canzonieri et al. reported a case of a 54-year-old woman patient without signs of tuberous sclerosis with three anatomically separated tumors in the same kidney. One was a typical angiomyolipoma, whereas the other two were renal cell carcinomas with a "fibroleiomuscular" component. The patient was alive and well 6 months later [5]. The largest series of these tumors was described by Kuhn et al., who described five cases of renal cell carcinomas with an angioleiomyoma-like proliferation [12]. Their patients included four women and one man aged 37–75 years. One patient died 3 years later with bone metastases, and no follow-up was provided for the remaining four patients [12]. Having reviewed figures of all above cited papers, we think that none of them described a tumor similar to the RAT. Specifically, no reported case reveals the typical snouts in the apical parts of the glandular structures, and none of the paper shows the basophilic nuclei alienated along the basal membrane producing the typical "shark' smile" arrangement. In addition, by the generosity of the authors, we were able to review a slide of the case published by Canzonieri et al. [5]. The stroma in their case seems to be unique, as it was much more fibrous with a "desmoplastic quality," much different from the "angioleiomyomatous" stroma in our cases or those published by Kuhn et al. [12].

RAT further differs in one clinical aspect from the renal cell tumors associated with angioleiomyomatous stroma published so far [5, 7, 11, 12]. While published cases of the latter shows a female predominance (seven out of eight patients) [5, 7, 11, 12], four out of the five patients with RAT in our series were males.

We are, however, aware of one possible case of RAT published recently. On the page 187, the authors of AFIP Fascicle 1 of "The Atlas of Tumor Pathology of Tumors of the Kidney, Bladder and Related Structures" show a putative mixed epithelial and stromal tumor of the kidney. Their Fig. 2-175 illustrates a lesion with branching adenomatous structures composed of basophilic nuclei alienated close to the basal membrane and having focally the same apical snouts as those in RAT. In addition, the rich capillary network rimming the adenomatous structures in their case seems to be identical to that seen in RAT [19]. We have never seen such an epithelial component in more than 40 cases of MESTKs in our files. Although no stroma is illustrated in the above figure of "MESTK" [19], we suppose that the stroma of the tumor must have been most probably angioleiomyomatous, being thus typical of RAT, rather than ovarian type stroma characteristic of MESTK [1, 16].

In the differential diagnosis, RAT should be distinguished from MESTK, angiomyolipomas, and clear renal cell carcinomas with angioleiomyomatous stroma. MESTK, in contrast to RAT, has a stroma, which is identical to ovarian stroma. In our experience with more than 40 cases of MESTK [14–16, 20, 23], pure leiomyomatous differen-

tiation in the ovarian stroma of MESTK is a rare finding, and if present, it looks as a focal metaplasia usually arising on the background of spindle cell ovarian stroma. MESTK further differs from RAT by the frequent occurrence of various Müllerian epithelial type differentiations including those of Fallopian tubal, endometrial, squamous ones [16] and even a variety with intestinal mucinous glandular epithelium revealing typical Paneth cells [23]. This mixture of various types of these Müllerian epithelia can often be seen within a single tumor mass in MESTK [16]. In addition, the ovarian stroma of MESTK can infrequently reveal fibrous areas indistinguishable from corpora albicantia [15], and rarely, there may even be lutein stromal cells identical to those seen in the ovaries [4]. Such epithelial and stromal features are never seen in RATs.

Angiomyolipomas differ from RAT by the presence of fat tissue and thick blood vessels devoid of elastic layer with the typical arrangement of the myoid stromal cells running perpendicularly to the lumina of these vessels. Most angiomyolipomas are associated with tuberous sclerosis complex, an association not observed with RATs. In addition, angiomyolipomas are usually devoid of glandular epithelial component, the exception being occasional renal cysts occurring especially in tuberous sclerosis patients. Immunohistochemically, angioleiomyomas react with melanocytic markers, especially with HMB45 practically in all cases. None of the melanocytic markers tested positive in the angioleiomyomatous stroma of RATs.

We further think that RAT differs from conventional clear cell carcinomas, which can rarely be associated with an identical leiomyomatous stroma occasionally forming abortive vascular structures. However, the epithelial component of RAT is entirely different from that in conventional clear cell carcinomas and is very distinctive, with basophilic nuclei arranged in typical rows and apical clear snouts resulting in the typical focal appearance of glandular structures to a "shark's smile." We have not encountered such an epithelial component in any of the 14,000 renal cell tumors in the Pilsen registry for kidney tumors. In addition, the VHL gene mutations, so common of conventional clear cell carcinomas, have not been found in any of the five cases of RAT. Immunohistochemically, CD10, which is a reliable marker of conventional clear cell carcinomas [3], was entirely negative in RAT, with the exception of one case wherein a small percentage of the neoplastic cells showed positive immunoreaction. Carbonic anhydrase IX cannot help in distinguishing RAT from clear cell renal carcinomas as both are positive. This antibody is, in our experience, rather nonspecific. Besides being reported to be present in many extrarenal neoplasms [2], it is seen in occasional cases of the papillary renal carcinoma [21]. In addition, it was reported to be positive in all cases recently reported clear cell papillary renal cell carcinomas, which the authors considered to be a distinct histopathologic and molecular genetic entity [6]. The immunopositivity of carbonic anhydrase IX of clear cell renal carcinoma, clear cell papillary renal cell carcinoma [21], and RAT is, however, interesting, because all these three tumor types reveal abundant clear cell cytoplasm within the epithelial component.

The last issue to discuss is the biological significance of RAT. In the original paper describing the tumor in 2000, we called it "benign renal angiomyoadenomatous tumor" [18]. In all four patients with RAT of the current series for whom the follow-up was available, the tumor behaved in a benign fashion. Histologically, all tumors looked benign. In spite of these facts, we contemporary removed the adjective "benign" from the name of the neoplasm until more cases with a long follow-up are available to meaningfully estimate their clinical behavior.

In summary, we describe five cases of a distinctive entity which we named as renal angiomyoadenomatous tumor. RAT was composed of typical epithelial component never seen in other tumors in our registry and angioleiomyomatous HMB45 negative stroma, which formed focally abortive vascular structures. Most cases of RATs in our series occurred in adult to old men (four of five), behaved in a benign fashion, and were not associated with tuberous sclerosis complex.

Acknowledgment The authors are grateful to Dr. Petr Mukensnabl for preparing excellent microscopical figures. This study was supported by grant IGA 9722-4

References

1. Adsay NV, Eble JN, Srigley JR, Jones EC, Grignon DJ (2000) Mixed epithelial and stromal tumor of the kidney. Am J Surg Pathol 24:958–970
2. Al-Ahmadie HA, Alden D, Qin L-X, Olgac S, Fine SW, Gopalan A, Russo P, Motzer RJ, Reuter VE, Tickoo ST (2008) Carbonic anhydrase IX expression in clear cel renal cell carcinoma. An immunohistochemical study comparing 2 antibodies. Am J Surg Pathol 32:377–382
3. Avery AK, Beckstead J, Renshaw AA, Corless CL (2000) Use of antibodies to RCC and CD10 in the differential diagnosis of renal neoplasms. Am J Surg Pathol 24:203–210
4. Buritica C, Serrano M, Zuluaga A, Arrabal M, Regauer S, Nogales FF (2007) Mixed epithelial and stromal tumour of the kidney with luteinised ovarian stroma. J Clin Pathol 60:98–100
5. Canzonieri V, Volpe R, Gloghini A, Carbone A, Merlo A (1993) Mixed renal tumor with carcinomatous and fibroleiomyomatous components, associated with angiomyolipoma in the same kidney. Pathol Res Pract 189:951–956
6. Gobbo S, Eble JN, Grignon DJ, Martignoni G, MacLennan GT, Shah RB, Zhang S, Brunelli M, Ceng L (2008) Clear cell papillary renal cell carcinoma. A distinct histopathologic and molecular genetic entity. Am J Surg Pathol 32:1239–1245
7. Govaerts JJL, van Gooswilligen JC, Vooys GP, Ramaekers FC, Herman CJ, Debruyne FM (1987) Renal hamartoma associated with renal cell (Grawitz) tumor. Eur Urol 13:276–280

8. Hes O, Michal M, Šulc M, Kočová L, Hora M, Rousarová M (1998) Glassy hyaline globules in granular cell carcinoma, chromophobe cell carcinoma and oncocytoma renal tumors. Anna Diagn Pathol 2:12–18
9. Hes O, Benákova K, Vaněček T, Šíma R, Michal M (2005) Clear cell type of renal cell carcinoma with numerous hyaline globules: A diagnostic pitfall. Pathol Intern 55:150–154
10. Hes O, Hora M, Vaněček T, Šulc M, Havlíček F, Michal M (2003) Conventional renal cell carcinoma with granulomatous reaction. A report of three cases. Virchows Archiv 443:220–221
11. Honey RJ, Honey RM (1977) Tuberous sclerosis and bilateral renal carcinoma. Br J Urol 49:441–446
12. Kuhn E, De Anda J, Manoni S, Netto G, Rosai J (2006) Renal cell carcinoma associated with prominent angioleiomyoma-like proliferation. Report of 5 cases and review of the literature. Am J Surg Pathol 30:1372–1381
13. Madewell JE, Goldman SM, Davis CJ, Hartman DS, Feigin DS, Lichtenstein JE (1983) Multilocular cystic nephroma. A radiographic-pathologic correlation of 58 patients. Radiology 146:309–321
14. Michal M, Syrůček M (1998) Benign mixed epithelial and stromal tumour of the kidney. Pathol Res Pract 194:445–448
15. Michal M (2000) Benign mixed epithelial and stromal tumor of the kidney. Pathol Res Pract 196:275–276
16. Michal M, Hes O, Bisceglia M, Simpson RW, Spagnolo DV, Parma A, Boudová L, Zachoval R, Suster S (2004) Mixed epithelial and stromal tumors of the kidney. A report of 22 cases. Virchows Archiv 445:359–367
17. Michal M, Vaněček T, Šíma R, Mukenšnabl P, Boudová L, Broučková M (2004) Primary capillary hemangioblastoma of peripheral soft tissues. Am J Surg Pathol 28:962–966
18. Michal M, Hes O, Havlíček F (2000) Benign renal angiomyoadenomatous tumor: A previously unreported renal tumor. Annals Diagn Pathol 4:311–315
19. Murphy WM, Grignon DJ, Perlman EJ (2004) AFIP atlas of tumor pathology (fourth series). Tumors of the kidney, bladder, and related urinary structures. American Registry of Pathology, Washington DC (Figure 2–175, 187 pp)
20. Švec A, Hes O, Michal M, Zachoval R (2001) Malignant mixed epithelial and stromal tumor of the kidney. Virchows Arch 439:700–702
21. Tu JJ, Chen Y-T, Hyjek E, Tickoo SK (2005) Carbonic anhydrase IX as a highly sensitive and specific marker of clear cell renal cell carcinoma: a comparative immunohistochemical study using a panel of commonly utilized antibodies in the differential diagnosis of renal cell tumors. Modern Pathol 18(suppl 1):169A
22. Widéhn S, Kindblom LG (1988) A rapid and simple method for electron microscopy of paraffin-embedded tissue. Ultrastruct Pathol 12:131–136
23. Yang Y, Hes O, Lanjing Z, Min L, Jian L, Min L, Hua W, Jie Z, Michal M (2005) Mixed epithelial and stromal tumor of the kidney with intestinal differentiation. A case report. Virchows Archiv 447:669–671